World Academy of Science, Engineering and Technology
International Journal of Mechanical and Mechatronics Engineering
Vol:10, No:10, 2016

Numerical Investigation of Electrohydrodynamics: Enhanced Heat Transfer in a Solid Sample

Suwimon Saneewong Na Ayuttaya

***Abstract*—**This paper presents a numerical investigation of electrically driven flow for enhancing convective heat transfer in a channel flow. This study focuses on the electrode arrangements, number of electrode and electrical voltage on Electrohydrodynamics (EHD) and effect of airflow driven on solid sample surface. The inlet airflow and inlet temperature are 0.35 m/s and 60 ºC, respectively. High electrical voltage is tested in the range of 0-30 kV and number of electrode is tested in the range of 1-5. The numerical results show that electric field intensity is depended on electrical voltage and number of electrode. Increasing number of electrodes is increased shear flow, so swirling flow is increased. The swirling flows from aligned and staggered arrangements are affecting within the solid sample. When electrical voltage is increased, temperature distribution and convective heat transfer on the solid sample are significantly increased due to the electric force much stronger.

***Keywords*—**Electrohydrodynamics, swirling flow, convective heat transfer, solid sample.

I. Introduction

A flow field under the influence of a combined electromagnetic field can be investigated by either of the two extreme models: EHD and Magnetohydrodynamics (MHD). The EHD model assumes a quasi-static electric field applied to a fluid containing electrically charged particles and the effect of magnetic field is negligible [1]. EHD effect is a branch of fluid mechanics concerned with electric force. When the electrical voltage is exposed to airflow, the airflow is created by ions generated in the corona discharge near the sharp electrode that drift to the ground in order to induce the shear flow. After that, swirling flow or secondary flow is appeared, so the momentum of airflow is enhanced [2]. From mechanism of EHD, the applications are divided into four groups. The first, second, third and fourth groups are increasing flow, spread flow, induced flow, and mixing process, respectively. For mixing process, the net effect of this secondary flow is the additional mixing of fluids and destabilization of boundary layer, therefore leading to a substantial increase in the heat transfer coefficients.

In order to improve the convective heat transfer, some researchers seriously studied in EHD flow control [3]-[7] and some researcher are mentioned EHD application for mixing process [8]-[10]. Green et al. [3] studied the electrokinetic manipulation of particles suspended in a fluid medium. The result showed that electric field could drive fluid flow where the temperature gradients were generated by the illumination source. The fluid flow pattern and frequency dependence were in accordance with the theory of electrothermal body forces. A qualitative explanation based on simple electric field geometry and a temperature gradient created through heating of the electrodes by the light adequately describes the experimental observations. Saneewong Na Ayuttaya et al. [7] numerically explored the influences of electrode arrangements and number of electrodes on the swirling flow under electric field. The results showed that when the gap became closer, size of swirling flow become smaller but vorticity was higher due to higher and denser electric field. The different elevation of electrode influenced the swirling flow direction. When the number of electrodes increased, electric field intensity increased. This causes the gradient of electrical voltage to be more increased, so the swirling flow becomes stronger.

From previous studies [6], [7], the improvement in the flow velocity is to increase the thermal efficiency and extend the heat transfer area, while minimum energy is consumed. Furthermore, EHD technique is utilized for controlling the patterns of airflow in order to enhance the convective heat transfer above sample surface because thermal boundary layer from material surface is damaged. In this study, the electric field effect on flow structure and swirling flow with EHD effect are investigated. The characteristics of swirling flow and heat transfer from two arrangements, i.e. aligned and staggered in a channel flow subjected to EHD for enhancing heat transfer in a solid sample are systematically investigated. Finally, electrical voltages are varied in order to studied temperature distribution within solid sample.

II. Mathematical Model

The mathematical models are developed to predict the electric field. The corona discharge occurs only in the vicinity around the electrode wire. The dielectric properties are constant and the effect of magnetic field is negligible. The governing equation of EHD -induced flow is then governed by Poisson's equation (1), the electric field strength (E) and conservation of space charge density (q) are defined by (2), (3) and (4), respectively:

$$\nabla \cdot \varepsilon \vec{E} = q \tag{1}$$

$$\vec{E} = -\nabla V \tag{2}$$

$$\nabla \cdot J = 0 \tag{3}$$

S. Saneewong Na Ayuttaya is with the Department of Mechanical Engineering, Chulachomklao Royal Military Academy, Nakhon-Nayok, Thailand, 26001 (e-mail: joysuwimon1@hotmail.com).

$$J = qb\vec{E} + q\vec{u} \tag{4}$$

where ε and J are dielectric permittivity and current density, respectively. The electric force per unit volume ($\vec{F}_E$) is the main driving force of corona-induced flow mixing. It is expressed as [11]:

$$\vec{F}_E = q\vec{E} - \frac{1}{2}\vec{E}^2\nabla\varepsilon + \frac{1}{2}\nabla\left[\vec{E}^2\left[\frac{\partial\varepsilon}{\partial\rho}\right]_T\rho\right] \tag{5}$$

For corona, discharge is appeared at room temperature and atmospheric pressure condition. The dielectric permittivity (ε) can be assumed to be constant. Therefore, the second and third terms on the right- hand side of (5) are negligible.

The mathematical models are developed to predict the flow field. The flow field is unsteady, single phase and incompressible flow. The fluid physical properties are assumed to be constant. The continuity equation (6) and Navier–Stokes equation (7) which coupled with Coulomb force equation can be written in the flowing form [7]:

$$\nabla\cdot\vec{u} = 0 \tag{6}$$

$$\rho\left[\frac{\partial\vec{u}}{\partial t} + (\vec{u}\cdot\nabla)\vec{u}\right] = -\nabla\vec{P} + \mu\nabla^2\vec{u} + \vec{F}_E \tag{7}$$

The mathematical models are developed to predict the heat transfer. Within a channel flow, the thermophysical properties are taken to be constant. The effect of buoyancy is negligible. No emission or absorption of radiant energy. Temperature distribution is calculated by energy equation (8). Within a solid sample, the governing equations describing the heat transfer within the sample is calculated from (9):

$$\rho C_p\left[\frac{\partial T}{\partial t} + \vec{u}\nabla T\right] = k\left(\nabla^2 T\right) \tag{8}$$

$$\frac{\partial T}{\partial t} = \alpha\nabla^2 T \tag{9}$$

where, C_p, k and α are the specific heat capacity, thermal conductivity and thermal diffusivity. In order to investigate the convective heat transfer enhancement (10) on the sample surface, the solid sample is placed under the bottom wall of channel flow and only the upper surface of is exposed to hot-airflow. So the convective heat transfer (h_c) is defined by the thermal equilibrium:

$$h_c = -\frac{k}{\Delta T}\frac{\partial T}{\partial n} \tag{10}$$

III. Computational Geometry and Boundary Condition

Fig. 1 shows a schematic view of three parts domain, the first, second and third parts are electric field, flow and heat transfer domains, respectively. Dimensions of three domains are 2.0 m long (L) × 0.15 m high (H). Electrode and ground are assumed to be a circle with a diameter of 0.5 mm. Position of ground is always fixed at x = 0 m and y = 0 m while the distances between electrode and ground in the horizontal (l) and vertical (h) directions or the gap are varied. For electrode arrangements, aligned arrangements (Fig. 1 (a)) and staggered arrangements (Fig. 1 (b)) are compared. The number of electrodes (n) and electrical voltages (V_0) are varied from 1 to 5 and 0 – 30 kV, respectively. A solid sample block (S) of 10 cm × 5 cm is placed at the lower wall and the top surface is exposed to the hot-airflow. Boundary condition of this problem is shown in Fig. 2. The inlet airflow ($u_i = 0.35\,m/s$) and the initial temperature ($T(t_0) = 60\,^{\circ}C$) of hot-airflow are assumed to be uniform. The initial temperature of sample ($T_s(t_0)$) is $25\,^{\circ}C$. The computational scheme is assembled in finite element model using a collocation method. This convergence test leads to the mesh with approximately 7000 elements.

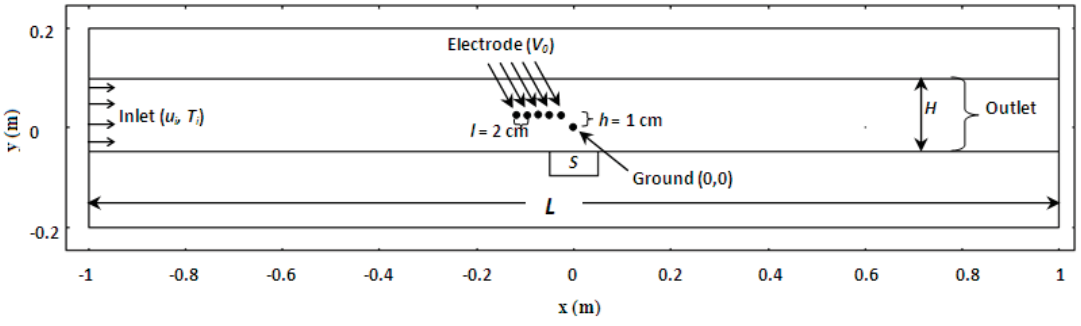

(a)

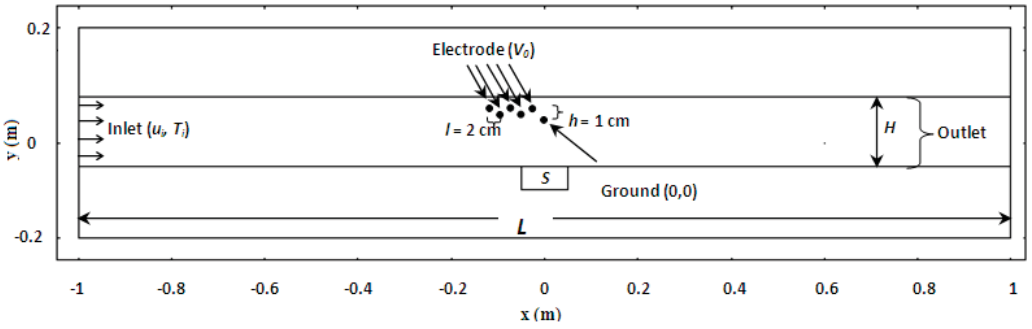

(b)

Fig. 1 A schematic view (a) aligned arrangements (b) staggered arrangements

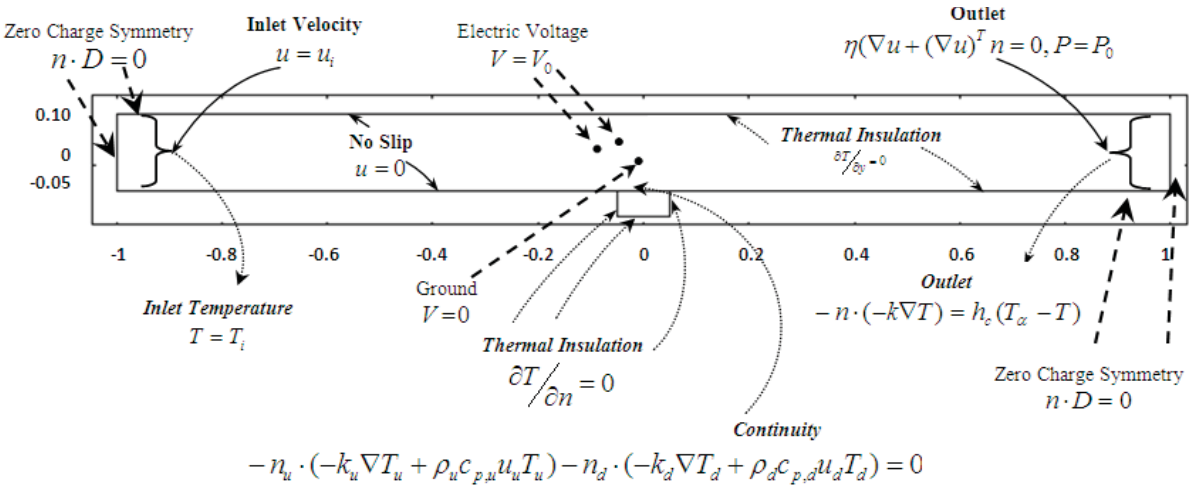

Fig. 2 Boundary conditions of electric field, flow field and temperature field used in analysis

IV. Results and Discussion

The properties of hot-airflow and solid sample are considered from Ramesh [12] and are shown in Table I and Table II, respectively.

TABLE I
SUBDOMAIN MODELING PARAMETER VALUES OF HOT-AIRFLOW [12]

Modeling parameter	Value
Ion mobility, b	$1.80 \times 10^{-4}\ m^2/V.s$
Initial temperature, $T(t_0)$	$60\ ^\circ C$
Dielectric permittivity, ε	$8.85 \times 10^{-12}\ F/m$
Kinematics viscosity, η	$1.76 \times 10^{-5}\ m^2/s$
Viscosity, μ	$1.97 \times 10^{-5}\ kg/m.s$
Density, ρ	$1.060\ kg/m^3$

TABLE II
SUBDOMAIN MODELING PARAMETER VALUES OF SOLID SAMPLE [12]

Modeling parameter	Value
Density of sample, ρ_s	$720 kg/m^3$
Initial temperature of sample, $T_s(t_0)$	$25\ ^\circ C$
Thermal conductivity of sample, k_s	$0.295\ W/(m.K)$

A. Electrode Arrangements on Fluid Flow Effect

The gap in the horizontal (l) and vertical (h) directions are fixed at 2 cm and 1 cm, respectively. The electrical voltage (V_0) is controlled at 10 kV and number of electrode (n) is 1. From Fig. 3, the maximum electrical voltage is appeared at the tip of electrode and the minimum electrical voltage is appeared at the tip of ground. Fig. 4 shows comparison of the swirling flow between No EHD (V_0=0 kV) and EHD (V_0=10 kV). In the case of No EHD (Fig. 4 (a)), air is flowed from the left to the right direction and the velocity of the air for a fully developed flow will be at its fastest at the center line of the channel flow. For the EHD case (Fig. 4 (b)), air is swirled in the counterclockwise direction when it moves in the electrode and ground zone. The maximum velocity is clearly displayed at the location closed to the lower wall so the upper of solid sample can easily disturbed by swirling flow. Pressure distribution is investigated from Fig. 5, when electric field is not included (No EHD) as shown Fig. 5 (a), pressure gradually decreases from the entrance to the exit. When electric field is introduced to flow (V_0=10 kV), as shown in Fig. 5 (b), the pressure is raised up around the electrode area. So the pressure ratio (maximum pressure with EHD to maximum pressure

without EHD) is proportional to square of electrical voltage, i.e. $\frac{P_{EHD}}{P_{NoEHD}} \propto V_0^{\,2}$, as shown from Fig. 6.

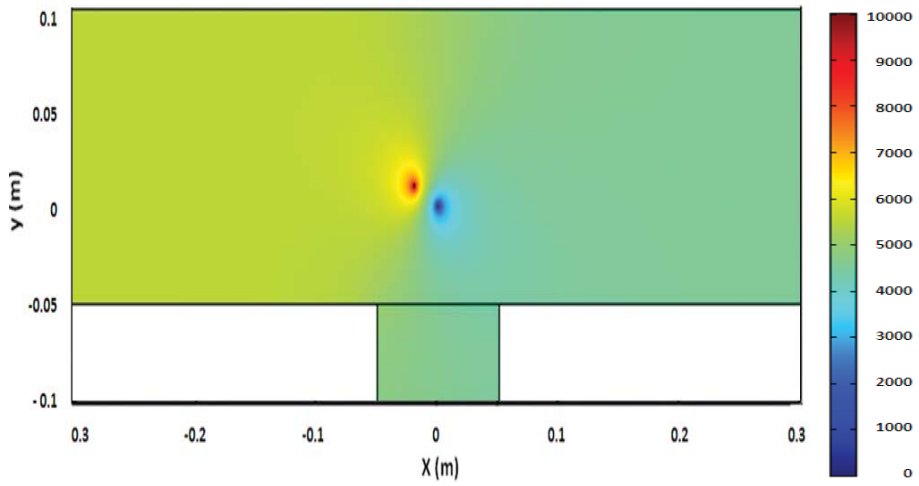

Fig. 3 Electrical voltage distribution when n=1, l =2 cm, h=1 cm, V_0=10 kV, and u_i =0.35 m/s

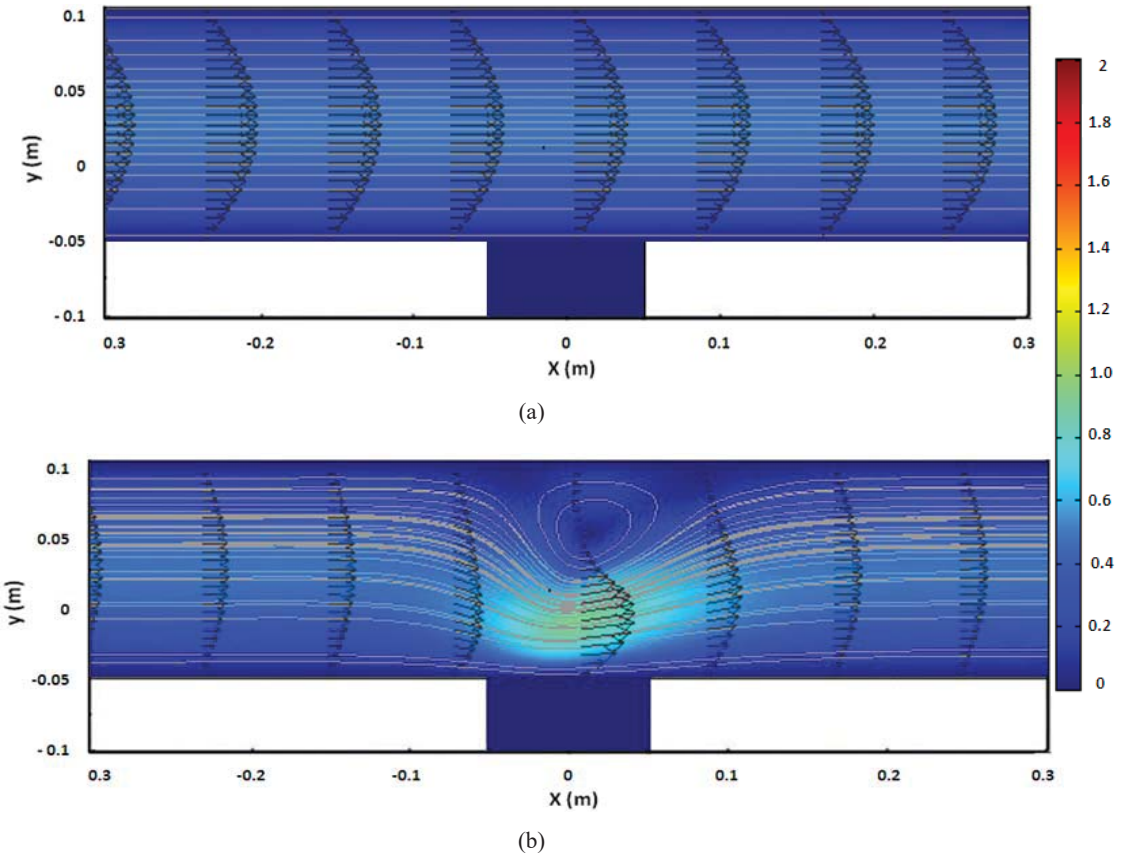

(a)

(b)

Fig. 4 Swirling flow with and without EHD when n = 1, l =2 cm, h=1 cm, and u_i =0.35 m/s (a) No EHD (b) V_0=10 kV

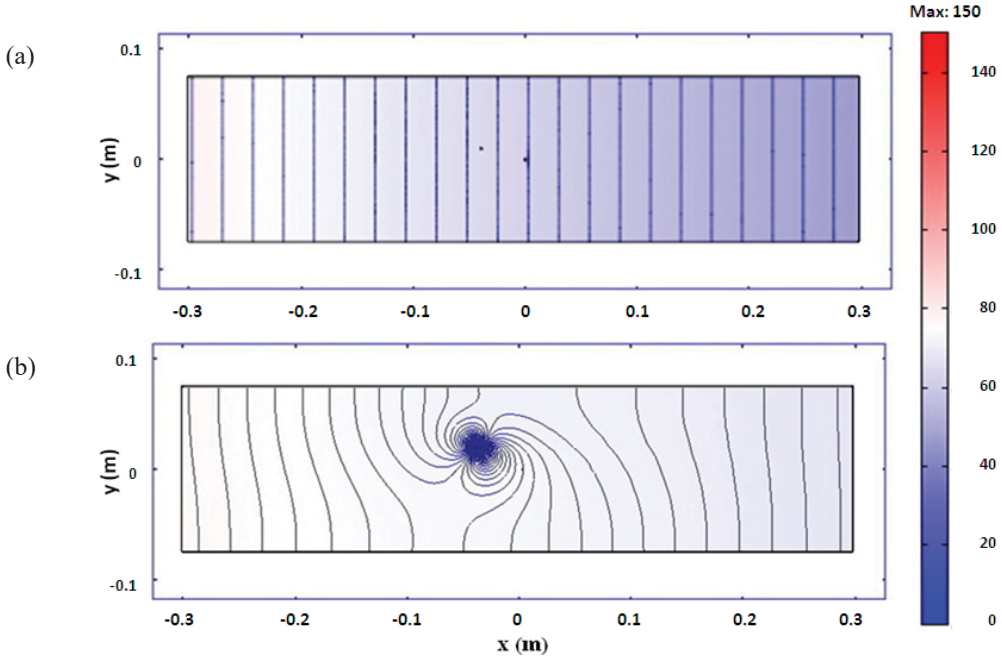

Fig. 5 Pressure distribution when l=2 cm, h=1 cm, and u_i = 0.35 m/s (a) No EHD (b) V_0=10 kV

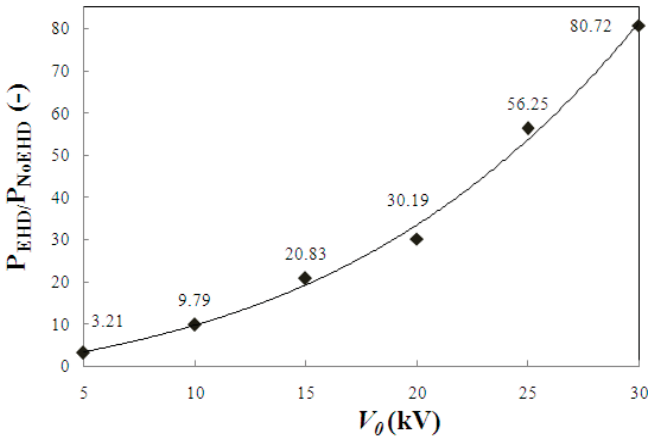

Fig. 6 Pressure ratio in various electrical voltages when l=2 cm, h=1 cm and u_i =0.35 m/s

In order to compare the fluid flow under the electric field, number of electrodes (n) is varied from 1 to 5, and electrode arrangements are studied for both of aligned arrangements and staggered arrangements. As addressed before, aligned arrangements and staggered arrangements are stalled in Figs. 1(a) and (b), respectively. The electrical voltage (V_0) is controlled at 10 kV. The gap is fixed at l = 2 cm and h = 1 cm. The gap of each electrode is 2 cm. Fig. 7 shows the electrical voltage distribution in the channel flow when number of electrodes (n) is 4. The electrical voltage zone of staggered arrangements (Fig. 7 (b)) is more expanded than aligned arrangements (Fig. 7 (a)). Due to arrangement of staggered arrangements can be disturbed to the electric field. Furthermore, electrical voltage distribution is increased with increasing number of electrodes, as shown in Figs. 3 and 7 (a).

Fig. 8 shows swirling flow in various number of electrode when aligned arrangements is investigated. The number of electrodes (n) of Figs. 8 (a) and (b) are 3 and 5, respectively. The result shows that, swirling flow from Fig. 8 (b) is widely swirled and extended more than that of swirling flow from Fig. 8 (a). Increasing number of electrode is increased shear flow, so swirling flow is increased

Fig. 9 shows swirling flow in various number of electrode when staggered arrangements are investigated. The number of electrodes (n) of Figs. 9 (a) and (b) are 3 and 5, respectively. It can be seen that the swirling flow from Fig. 9 is the same trend with Fig. 8. By the swirling flow from staggered arrangements (Fig. 9) is widely swirled and extended more than that of aligned arrangements (Fig. 8) but swirling flow from aligned arrangements is more violent. From Fig. 10, the velocity ratio is compared in various number of electrode (n) and the velocity ratio is defined as maximum velocity with EHD to maximum velocity without EHD, i.e. u_{EHD} / u_{NoEHD}. The variation of electrode number (n) is treated with parabolic function. When number of electrode is controlled, velocity ratio of aligned arrangements is higher than staggered arrangements. Fig. 11 shows the velocity ratio is increased with increasing electrical voltage. The variation of electrical voltage (V_0) is treated with straight function. When number of electrode is controlled, the velocity ratio of aligned arrangements is higher than staggered arrangements. When electrode arrangement is controlled, velocity ratio of n=5 is higher than velocity ratio of n=3. It can be seen that number of electrode is more influenced than electrode arrangement.

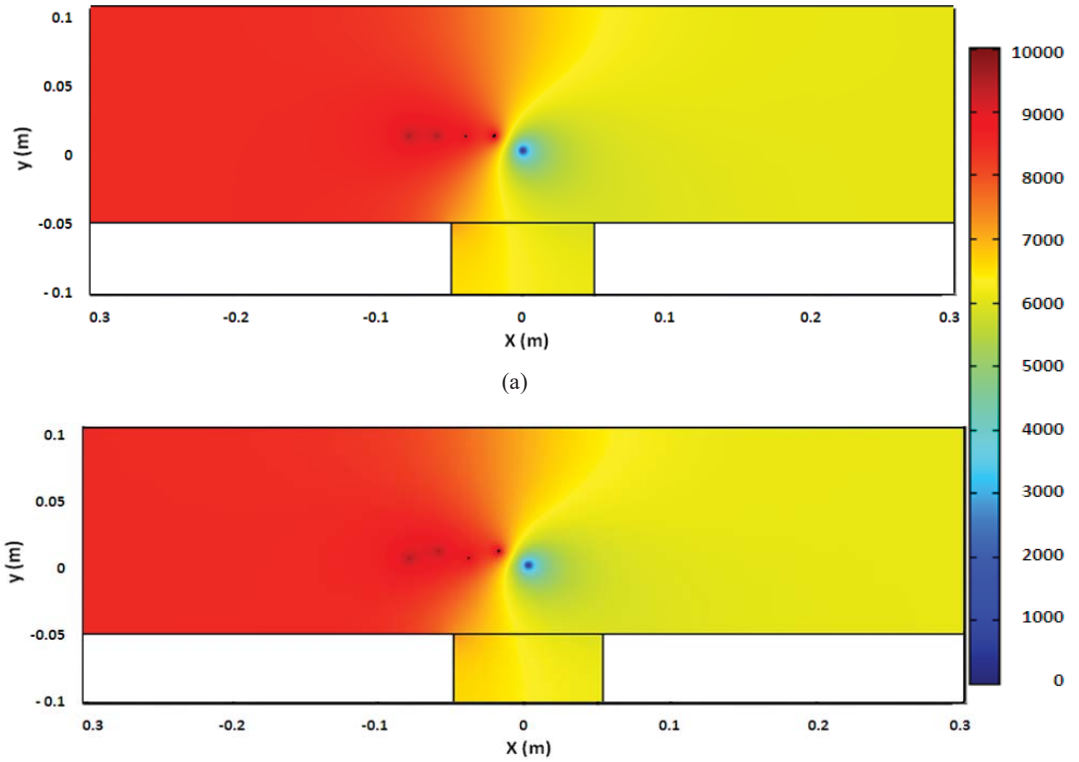

(a)

(b)

Fig. 7 Electrical voltage distribution when V_0 = 10 kV and u_i = 0.35 m/s (a) n = 4 of aligned arrangements and (b) n = 4 of staggered arrangements

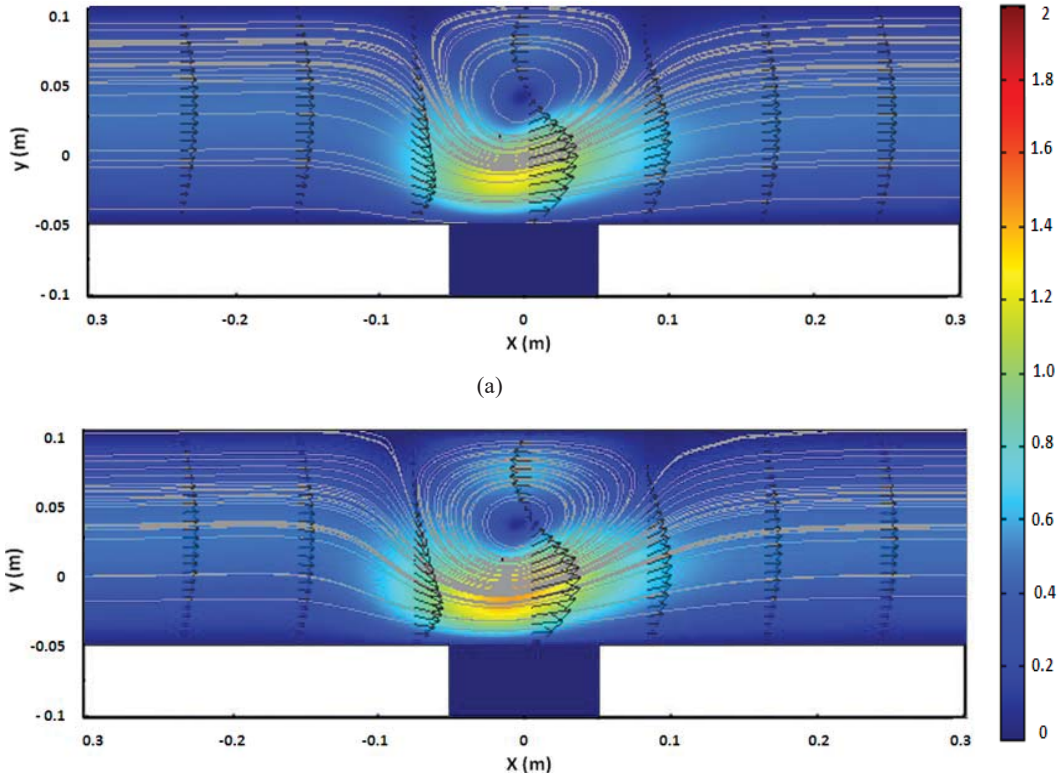

(a)

(b)

Fig. 8 Swirling flow in various n of aligned arrangements (a) n=3 (b) n=5 when V_0=10 kV, and u_i =0.35 m/s

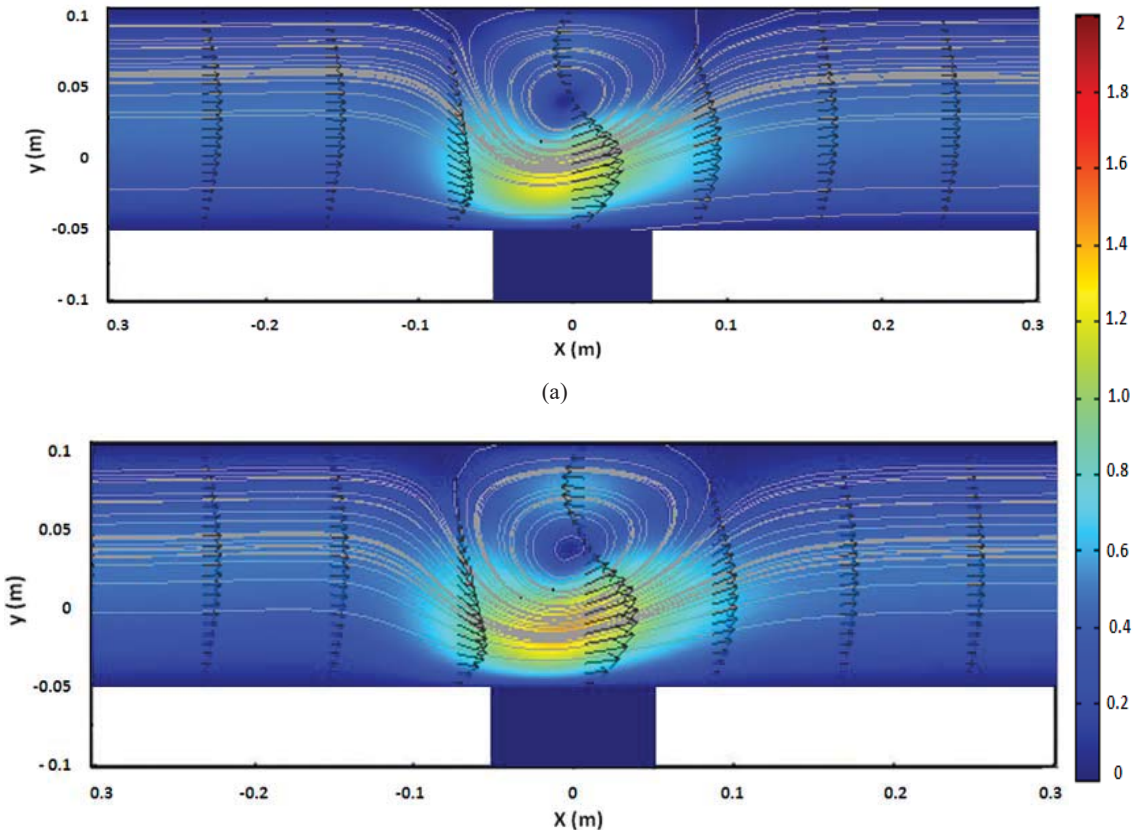

(a)

(b)

Fig. 9 Swirling flow in various n of staggered arrangements (a) n=3 (b) n=5 when h=1 cm, l=2 cm, V_0=10 kV, and u_i =0.35 m/s

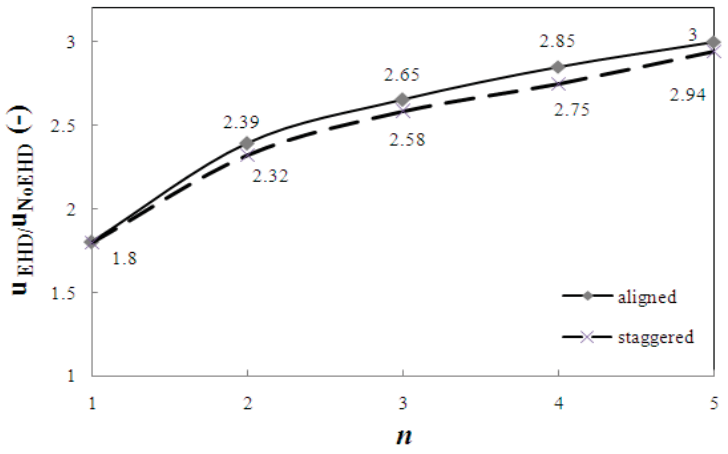

Fig. 10 Comparison of velocity ratio between aligned arrangements and staggered arrangements in various n when h=1 cm, l=2 cm, V_0=10 kV and u_i =0.35 m/s

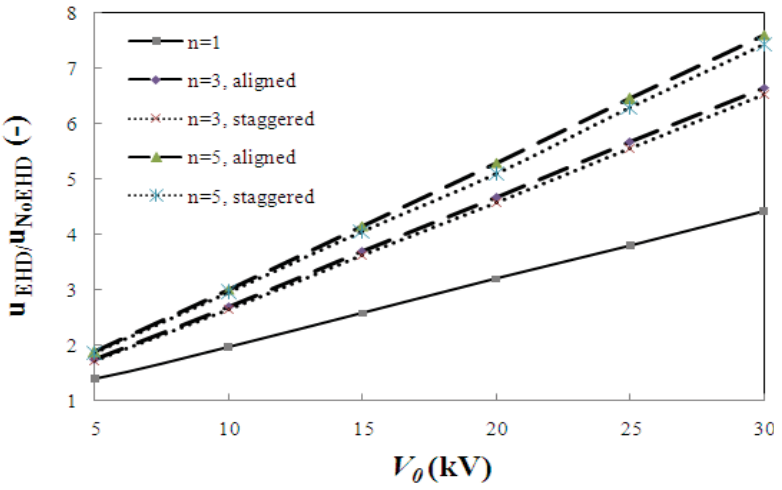

Fig. 11 Comparison of velocity ratio between aligned arrangements and staggered arrangements in various *n* and V_0 when u_i = 0.35 m/s

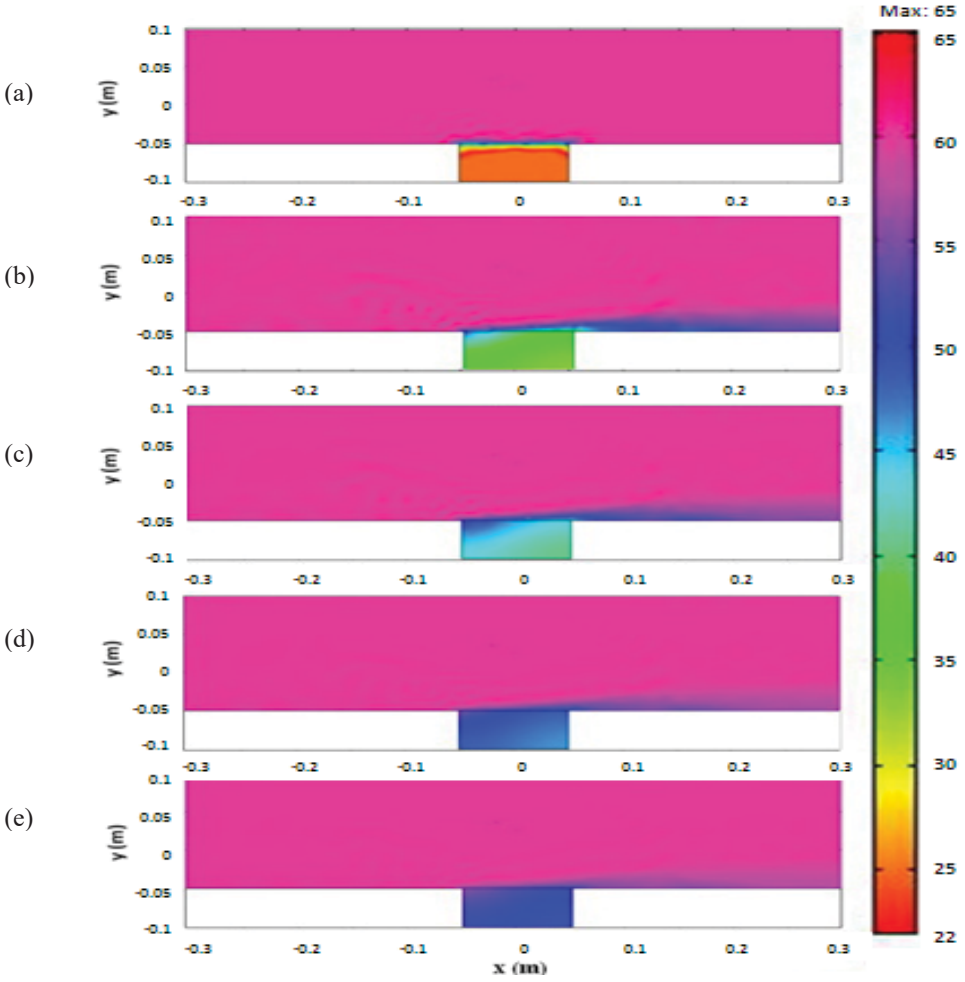

Fig. 12 Temperature distribution in channel flow and within a solid sample with *l*= 2 cm and *h*=1 cm in various times when V_0=20 kV and u_i =0.35 m/s (a) t=0 s (b) t=1800 s (c) t=3600 s (d) t=5400 s and (e) t =7200 s

B. Electrode Arrangements for Enhancing the Convective Heat Transfer on Solid Sample

In order to study temperature distribution (isotherm line) in channel flow and within solid sample, the inlet airflow (u_i) is 0.35 m/s. The gap is fixed at *l* = 2 cm and *h* = 1 cm. The electrical voltage (V_0) is controlled at 20 kV and number of electrode (*n*) is 1. Temperature distribution (isotherm line) in channel flow and within sample is considered in Fig. 12. It can

be seen that temperature within the solid sample is increased with increasing times. Fig. 13 shows the temperature distribution within the solid sample in various electrical voltage t = 1 hr. With no effect of swirling flow, hot-airflow is influenced with solid sample surface as shown in Fig. 13 (a). With swirling flow effect, electrical voltage of Figs. 13 (b), (c) and (d) are 10, 20 and 30 kV, respectively. Fluid flow above the sample surface is faster and then leads the heat to more transfer to the solid sample surface. This results the temperature of a solid sample to rapidly increase.

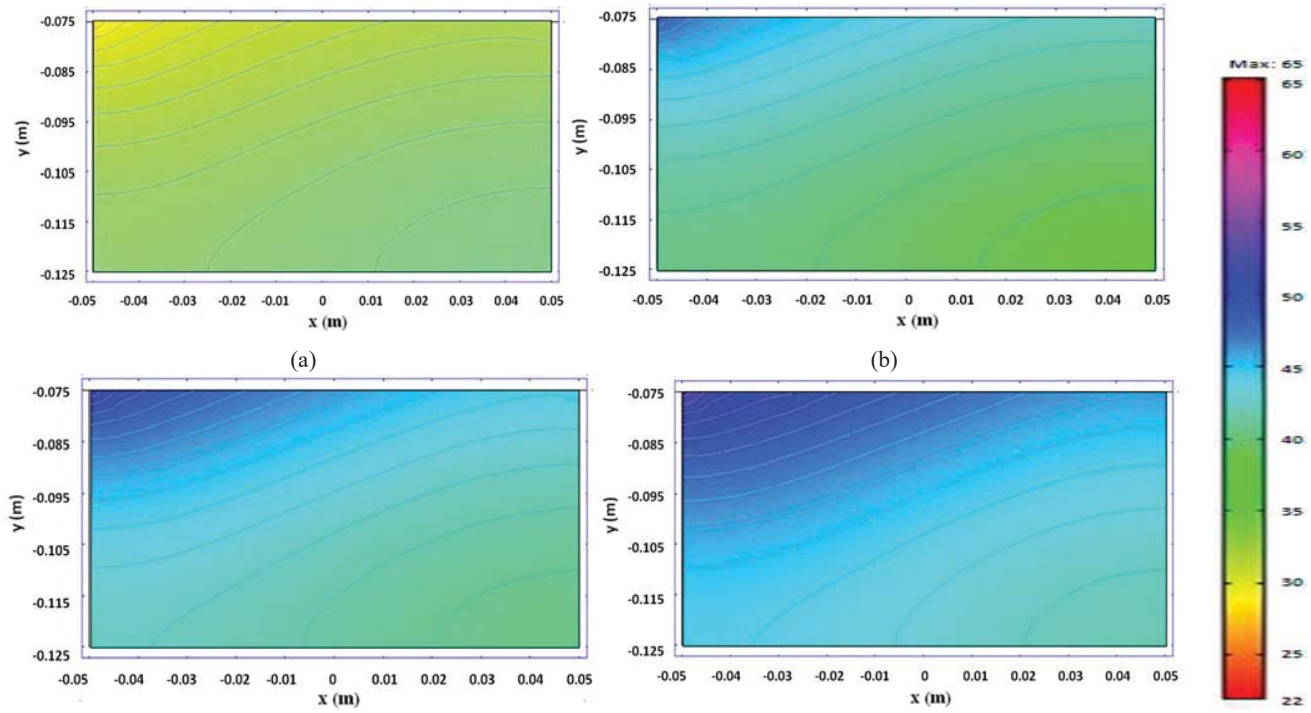

Fig. 13 Temperature distribution within a solid sample in various electrical voltages when l=2 cm, h=1 cm, u_i =0.35 m/s and t=1 hr (a) V_0=0 kV (b) V_0=10 kV (c) V_0=20 kV and (d) V_0=40 kV

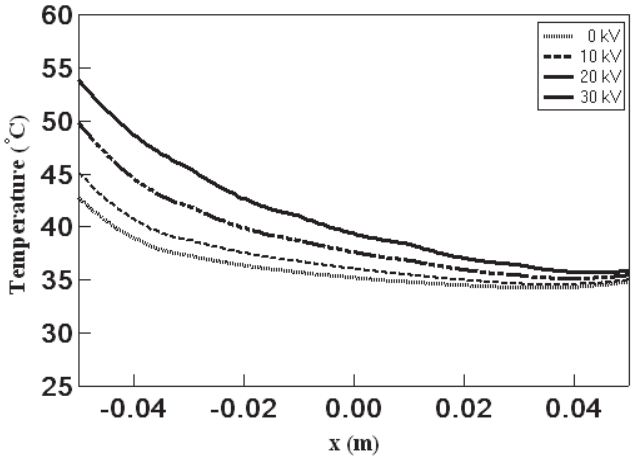

Fig. 14 Comparison on temperature of the solid sample surface in various electrical voltages when l=2 cm, h=1 cm, u_i =0.35 m/s and t=1 hr

From increasing electrical voltage, temperature from solid sample surface is increased as shown in Fig. 14. Due to the non-uniform heat flux on sample surface, the temperature distribution in solid sample is not uniform. The left of temperature from the solid sample surface are higher than the right because swirling flow is circulated in counterclockwise direction (supplied from the left to the right direction). In order to study the convective heat transfer ratio under electric field, electrode number (n) is varied from 1 to 5. Electrode arrangements are studied both of aligned and staggered arrangements. Electrical voltage (V_0) is varied from 0 to 30 kV. The convective heat transfer ratio is defined as maximum convective heat transfer coefficient with EHD to maximum convective heat transfer coefficient without EHD, i.e. $\overline{h}_{EHD} / \overline{h}_{NoEHD}$. The gap is fixed at l = 2 cm and h = 1 cm, respectively. The gap of each electrode is 2 cm and t = 1 hr. In case of aligned arrangements, the variations of number of electrodes (n) are treated with parabolic function as shown in Fig. 15. When V_0 = 5 kV, the convective heat transfer ratio is not different in various number of electrodes and it is gradually increased when electrical voltage is increased. The trend of convective heat transfer ratio from staggered arrangements is the same trend with aligned arrangements. But trend of convective heat transfer ratio from aligned arrangements (Fig. 15) is steeper than that case of convective heat transfer ratio from staggered arrangements (Fig. 16). With increasing number of electrodes and increasing electrical voltage, aligned arrangements are more influenced than

staggered arrangements. From Fig. 17, the convective heat transfer ratio is increased with increasing electrical voltage. When n = 3, the convective heat transfer ratio of aligned arrangements is higher than staggered arrangements When electrode arrangement is controlled, convective heat transfer ratio of n = 5 is higher than n = 3. It can be seen that number electrode is more influenced than electrode arrangements. In addition, the convective heat transfer ratio is dominated with high electrical voltage. The convective heat transfer ratio is proportional to square of electrical voltage, i.e. $\frac{\bar{h}_{EHD}}{\bar{h}_{NoEHD}} \propto V^2$.

V. Conclusion

(1) The swirling flow from staggered arrangements is widely swirled and extended more than that of aligned arrangements, but swirling flow and convective heat transfer from aligned arrangements is more violent.
(2) Increasing number of electrode and electrical voltage are increased shear flow, so swirling flow and convective heat transfer are increased.
(3) When number of electrode is controlled, velocity ratio of aligned arrangements is higher than staggered arrangements. This is because electric field is more concentrated and arrangement can support swirling flow direction.
(4) When increasing electrical voltage, temperature from solid sample surface is increased and the convective heat transfer ratio is increased with increasing electrical voltage.

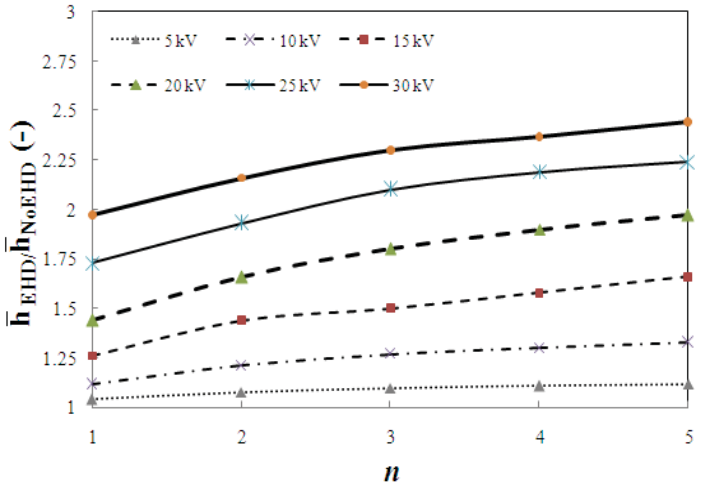

Fig. 15 Convective heat transfer ratio of aligned arrangements in various n and V_0 when u_i = 0.35 m/s and t=1 hr

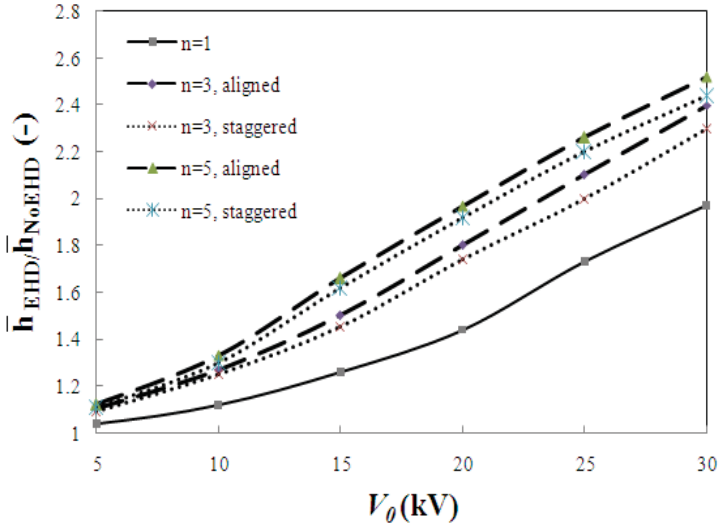

Fig. 16 Convective heat transfer ratio of staggered arrangements in various n and V_0 when u_i = 0.35 m/s and t=1 hr

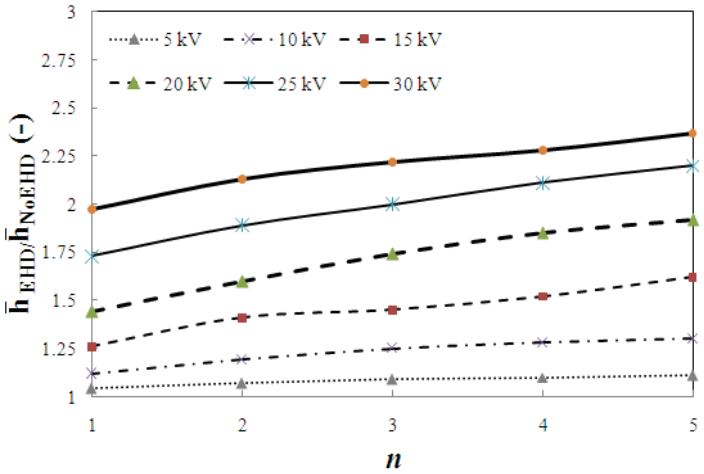

Fig. 17 Convective heat transfer ratio between aligned arrangements and staggered arrangements in various *n* and V_0 when u_i = 0.35 m/s and t=1 hr

ACKNOWLEDGMENT

This work has been financially supported by the Thailand Research Fund (TRG5780066) and Chulachomklao Royal Military Academy for their support of this study.

REFERENCES

[1] G. S. Dulikravich, V. Ahuja and S. Lee, "Modeling of dielectric fluid solidification with charged particles in electric fields and reduced gravity," *Numerical Heat Transfer, Part A*., vol. 25, pp. 357-373, 1994.
[2] A. Yabe, Y. Mori and K. Hijikata, "Active heat transfer enhancement by utilizing electric fields," *Annual Reviews of Heat Transfer*., vol.7, pp. 193-244, 1996.
[3] N. G. Green, A. Ramos, A. Gonzalez, A. Castellanos and H. Morgan, "Electric field induced fluid flow on microelectrodes: the effect of illumination," *Journal of Physics D: Applied Physics*., vol. 33(2), pp. 13-17, 1999.
[4] W. D. Ristenpart, I. A. Aksay and D. A. Saville, "Assembly of colloidal aggregates by electrohydrodynamic flow: kinetic experiments and scaling analysis," *Physical Review*., vol. 69, pp. 021405-1-021405-8, 2004.
[5] N. Takeuchi, K. Yasuoka and S. Ishii, "Inducing mechanism of electrohydrodynamic flow by surface barrier Discharge," *IEEE Transactions on Plasma Science*, vol. 35(6), pp. 1704-1709, 2007.
[6] G. Tomar, D. Gerlach, G. Biswas, N. Alleborn, A. Sharma, F. Durst, S. W. J. Welch and A. Delgado, "Two-phase electrohydrodynamic simulation using a volume-of-fluid approach," *Journal of Computational Physics*, vol. 227, pp. 1267-1285, 2007.
[7] S. Saneewong Na Ayuttaya, C. Chaktranond and P. Rattanadecho, "Numerical analysis of influence of electrode position on fluid flow in a 2-D rectangular duct flow," *Journal of Mechanical Science and Technology*, vol. 27(7), 1957-1962, 2013.
[8] D. B. Go, A. Maturana, T. S. Fisher and S. V. Garimella, "Enhancement of external forced convection by ionic wind," *Internal Journal of Heat and Mass Transfer*, vol. 51, pp. 6047-6053, 2008.
[9] C. Chaktranond and P. Ratanadecho, "Analysis of heat and mass transfer enhancement in porous subjected to electric fields (effects of particle sizes and layered arrangement)," *Experimental Thermal and Fluid Science*, vol. 34, pp. 1049-1056, 2010.
[10] N. Sharma, G. Diaz and E. Leal-Quirós, "Electrolyte film evaporation under the effect of externally applied electric field," *International Journal of Thermal Sciences*, vol. 68, pp. 119-126, 2013.
[11] L. D. Landau and E. M. Lifshitz, "Electrohydrodynamics of Continuous Media," Pergamon, New York, 1963.
[12] M. N. Ramesh, "Effect of cooking and drying on the thermal conductivity of rice," *International Journal of Food Properties*, vol. 3(1), pp. 77-92, 2000.

S. Saneewong Na Ayuttaya received Ph.D. degree from the Department of Mechanical Engineering, Thammasat University, Rangsit Campus, Thailand, in 2013. Her research interests are enhancement of heat and mass transfer in Electrohydrodynamics technique, numerical and experimental investigation of heat and mass transfer in saturated and unsaturated porous media.